



Inferring the demographic history of an oligophagous grasshopper: Effects of climatic niche stability and host-plant distribution



Víctor Noguerales^{a,*}, Pedro J. Cordero^a, Joaquín Ortego^b

^a Grupo de Investigación de la Biodiversidad Genética y Cultural, Instituto de Investigación en Recursos Cinegéticos – IREC (CSIC, UCLM, JCCM), Ronda de Toledo 12, E-13071 Ciudad Real, Spain

^b Department of Integrative Ecology, Estación Biológica de Doñana (EBD-CSIC), Avda. Américo Vespucio 26, E-41092 Seville, Spain

ARTICLE INFO

Keywords:

Climatic stability
Ecological niche modelling
Genetic diversity
Genetic structure
Host-plant association
Northern refugia

ABSTRACT

Understanding the consequences of past environmental changes on the abiotic and biotic components of the landscape and deciphering their impacts on the demographic trajectories of species is a major issue in evolutionary biogeography. In this study, we combine nuclear and mitochondrial genetic data to study the phylogeographical structure and lineage-specific demographic histories of the scrub-legume grasshopper (*Chorthippus binotatus binotatus*), a montane taxon distributed in the Iberian Peninsula and France that exclusively feeds on certain scrub-legume species. Genetic data and paleo-distribution modelling indicate the presence of four main lineages that seem to have diverged in allopatry and long-term persisted in Iberian and French refugia since the Mid Pleistocene. Comparisons of different demographic hypotheses in an Approximate Bayesian Computation (ABC) framework supported a population bottleneck in the northwestern French clade and paleo-distribution modelling indicate that the populations of this lineage have experienced more severe environmental fluctuations during the last 21 000 years than those from the Iberian Peninsula. Accordingly, we found that nuclear genetic diversity of the populations of scrub-legume grasshopper is positively associated with local stability of suitable habitats defined by both Pleistocene climate changes and historical distributional shifts of host-plant species. Overall, our study highlights the importance of integrating the potential effects of abiotic (i.e. climate and geography) and biotic components (i.e. inter-specific interactions) into the study of the evolutionary and demographic history of specialist taxa with narrow ecological requirements.

1. Introduction

Quaternary climatic fluctuations have reshaped the distribution of worldwide biotas and impacted the demographic trajectories of most organisms (Hewitt, 2004a, 2011). In Europe, the prevailing paradigm establishes that most species responded to cooling phases by southern distributional shifts and survival in glacial refugia predominantly located in Mediterranean peninsulas that maintained the source populations from which northern areas were re-colonized during interglacial periods (Hewitt, 1999; Schmitt, 2007). Many empirical (Hewitt, 2004b; Cornille et al., 2013) and theoretical studies (Excoffier and Ray, 2008; Arenas et al., 2012) have analyzed the genetic footprints of such distributional shifts and demonstrated the validity of the expansion-contraction model to explain patterns of genetic diversity and structure in many organisms (Taberlet et al., 1998; Provan and Bennett, 2008). The refugia hypothesis has been invoked as an excellent conceptual framework to understand why populations from areas experiencing long-term climatic stability harbor a higher and unique genetic diversity in

comparison with those from regions submitted to more climate instability (Carnaval et al., 2009; Yannic et al., 2014). Nevertheless, most research on this topic has focused on temperate species and the specific predictions of the expansion-contraction model may not be valid for montane or cold-adapted species (Galbreath et al., 2009; Ricanova et al., 2013). Species adapted to cool environments are likely to have experienced range expansions and higher connectivity among populations in glacial periods and persisted forming isolated populations in interglacial refugia during warming phases (Willis and van Andel, 2004; Galbreath et al., 2009). Accordingly, a growing body of literature is yielding strong evidence about many species that survived in cryptic refugia located in the northernmost areas of their present-day distribution (Stewart and Lister, 2001; Stewart et al., 2010). In comparison with southern refugia, northern refugia are less predictable through time and space and, therefore, the impacts of climate-driven changes in landscape composition on the demography of cool-adapted species are still poorly understood (Vega et al., 2010; Parducci et al., 2012).

Beyond the importance of past environmental fluctuations, the

* Corresponding author.

E-mail address: victor.noguerales@csic.es (V. Noguerales).

<http://dx.doi.org/10.1016/j.ympev.2017.10.012>

Received 28 March 2017; Received in revised form 9 September 2017; Accepted 22 October 2017

Available online 26 October 2017

1055-7903/ © 2017 Elsevier Inc. All rights reserved.

distribution and abundance of a species are often shaped by many other ecological processes that are not necessarily captured by its climatic niche envelop (Mouritsen and Poulin, 2002; Hampe, 2004). This is the case of many specialist organisms whose demography is expected to be determined not only by changes in the spatial distribution of climatically suitable areas but also by range shifts experienced by the hosts on which they depend for feeding or development (e.g. Tsai and Manos, 2010; Cangi et al., 2013; Kuhn et al., 2016). Climate-based distributional shifts of host species can have a considerable impact on specialist taxa, particularly if differences in species-specific environmental tolerances result in the responses to climate change of the latter inferred on the basis of bioclimatic niche models are largely uncoupled from those experienced by their hosts (Tsai and Manos, 2010; Borer et al., 2012). This can lead to some species are not able to persist in regions falling within its optimal climate niche if their host-taxa are absent and, conversely, they may maintain viable populations in climatically sub-optimal areas as long as they sustain stable or abundant host populations (Jackson and Overpeck, 2000; Criscione and Blouin, 2004). Under this scenario, it would be expected that population genetic connectivity and persistence are shaped by the combined stability of suitable habitats for both the focal taxon and its hosts and that the impact of the latter is more pronounced in specialist species exclusively dependent on one or a few host taxa (Laukkanen et al., 2014). A biologically realistic approach would be to integrate information on the climate niche of the focal species (as a proxy of fundamental niche concept) and well-understood ecological relationships with host taxa (as a proxy of realized niche concept) (Hutchinson, 1957; Wharton and Kriticos, 2004; Freeman and Mason, 2015). This approach can potentially offer a more comprehensive picture about the demographic history of a species and how it is being shaped by the abiotic and biotic components of the landscape (Jackson and Overpeck, 2000; Svenning et al., 2011). A number of studies have addressed the potential negative impacts of ongoing climate change on biodiversity as a consequence of spatio-temporal mismatches in distributional shifts between host-plants and their specialist herbivores (e.g. Schweiger et al., 2008). However, studies looking backward in time to analyze the impacts of Pleistocene distributional shifts of host-plants on the population dynamics of their associated phytophagous taxa are almost absent (for an exception see Tsai and Manos, 2010).

The scrub-legume grasshopper, *Chorthippus binotatus binotatus* (Charpentier, 1825) (Orthoptera: Acrididae), is a well-suited study system to analyze the influence of Quaternary climatic fluctuations on the demographic history of a phytophagous species presenting narrow ecological requirements. This taxon is distributed throughout France, Spain and Portugal (Defaut, 2011) and occupies primarily montane habitats between 900 and 2500 m.a.s.l., often forming highly isolated populations separated by unsuitable low elevation areas (Noguerales et al., 2017). The scrub-legume grasshopper can be also exceptionally found at low elevations (even at sea level) near to the Atlantic coast, where it forms small populations in highly isolated patches of suitable habitat (Picaud et al., 2003; Platz and Cloupeau, 2010). Quaternary climatic fluctuations are likely to have strongly impacted the genetic structure of this species, whose populations are expected to have persisted in high elevation and cold refugia during interglacials and experienced regional expansions during glacial periods. The scrub-legume grasshopper is an oligophagous taxon linked to certain scrub-legume communities on which it depends for feeding and refuge (Llucà-Pomares, 2002; Picaud et al., 2002; Defaut, 2011). Specifically, this grasshopper exclusively feeds on thirteen scrub-legume species belonging to very closely related genera (*Cytisus*, *Echinospartum*, *Erinacea*, *Genista* and *Ulex*) from the tribe *Genisteae* (Llucà-Pomares, 2002; Defaut, 2011 and references therein; V.N., P.J.C. and J.O., pers. obs.). Plant species of this tribe can be found up to 2500 m.a.s.l. and exhibit important differences in their specific ecological requirements although they share a general preference for montane and cool habitats. Nowadays, some of these scrub species are widely distributed taxa, such as

Cytisus scoparius or *Ulex europaeus*, whose ranges span entire continental Europe, whereas other species are narrow endemics exclusively distributed in certain mountain ranges (e.g. *Echinospartum bardanessi*, *E. boissieri*, *E. horridum* or *Genista versicolor*) (Talavera et al., 2001). For these reasons, it is expected that the past demography of the scrub-legume grasshopper has been shaped by spatiotemporal changes in both the abiotic (i.e. climate regimes, geography) and biotic (i.e. host-plant distributional shifts) components that jointly define the ecological requirements of the species.

Here, we employ an integrative approach aimed to disentangle the evolutionary history and past demography of scrub-legume grasshopper across its entire distribution range. To this end, we combined nuclear and mitochondrial genetic data with paleo-distribution modelling to determine the stability of climatically suitable areas for both the grasshopper and its host-plant species and infer lineage-specific demographic histories from the genetic footprints left by past population size changes and distributional shifts. First, we used phylogenetic and Bayesian clustering analyses to determine the phylogeographic genetic structure of the scrub-legume grasshopper, estimate divergence times among the main lineages, and identify areas of long-term population persistence (i.e. refugia). Specifically, we tested whether northern populations are the outcome of range expansions from the Iberian Peninsula during favorable periods (i.e. “southern refugium and expansion” hypothesis) or if they conform lineages that have evolved *in situ* and long-term persisted into micro-refugia (i.e. “cryptic northern refugium” hypothesis) (Hickerson and Cunningham, 2005; Parducci et al., 2012). Second, given that different demographic events (such as range expansions or bottlenecks) can leave similar signatures on patterns of genetic diversity and structure (Falush et al., 2016), we used an Approximate Bayesian Computation (ABC) framework to formally compare different demographic scenarios. Finally, we tested whether the spatial distribution of genetic diversity in the scrub-legume grasshopper is explained by the geographic location of stable areas sustaining longstanding host-plant communities (Tsai and Manos, 2010; Laukkanen et al., 2014) and/or climatically suitable habitats for our focal species (Carnaval et al., 2009; Yannic et al., 2014).

2. Material and methods

2.1. Population sampling

Between 2012 and 2014, we collected 794 individuals from 55 populations of scrub-legume grasshopper, *Chorthippus binotatus binotatus* (Charpentier, 1825). These populations span the entire European distribution range of the species (~900,000 km², see Fig. S1) according to our own surveys and occurrence-data available in the literature (Llucà-Pomares, 2002; Defaut, 2011). Population codes and further information on sampling locations are given in Table S1.

2.2. Microsatellite data and estimates of genetic diversity

We employed a salt extraction protocol to purify genomic DNA from a hind leg of each specimen (Aljanabi and Martinez, 1997). All specimens were genotyped at 18 polymorphic microsatellites markers whose characteristics and PCR cycling conditions are described in Basiita et al., 2016. We performed PCR amplifications and genotyping as described in Ortego et al., 2015a. We tested for deviations from Hardy-Weinberg equilibrium (HWE), linkage disequilibrium (LD) and the presence of null alleles following the procedure described in Noguerales et al. (2016a). Six loci (Cbin08, Cbin16, Cbin36, Cbin50, Cbin56 and Cbin57) were discarded from all downstream analyses because of HW disequilibrium in all populations and the presence of null alleles. We did not find evidence for linkage disequilibrium between any pair of loci in any sampling population after sequential Bonferroni corrections (Rice, 1989).

We estimated nuclear genetic diversity for populations with ≥ 9

genotyped individuals. As estimates of population genetic diversity, we used allelic richness (A_R) standardized for sample size and expected heterozygosity (H_E), calculated as implemented in HP-Rare (Kalinowski, 2005) and Arlequin 3.5 (Excoffier and Lischer, 2010), respectively. For illustrative purposes, population genetic diversity was displayed in a map by conducting a spatial interpolation of A_R and H_E values using the Inverse Distance Weight (IDW) function available in ArcGIS 10.3 (ESRI, Redlands, CA, USA).

2.3. Mitochondrial DNA data and estimates of genetic diversity

We aimed to amplify a fragment of the mitochondrial cytochrome oxidase subunit I (COI) gene for a maximum of eight randomly selected specimens per population. However, we got non-resolvable electropherograms and/or very short sequences for a high number of individuals and populations. Finally, we successfully recovered high-quality sequences (with an average length of 619 bp) for 219 individuals from 45 populations spanning the entire distribution range of the species (Table S1). PCR reactions were performed in 15 μ l volumes using the universal primers LCO1490 and HCO2198 (Folmer et al., 1994) and with the same reagents and PCR program than for microsatellite markers, but using an annealing temperature of 50 °C. Amplified products were commercially purified and sequenced (Macrogen, South Korea). We edited, removed the primers and trimmed all sequences to the same length (552 bp) using Sequencher 4.10.1 (GeneCodes Corporation, Ann Arbor, MI, USA). The sequences were aligned using ClustalW web-service (www.genome.jp/tools/clustalw/). None of the sequences had premature stop codons and were deposited in GenBank with accession numbers KY709453–KY709671.

For sampling locations with ≥ 4 sequenced individuals for COI, we used DnaSP 5.10 (Librado and Rozas, 2009) to calculate different population genetic diversity indices including number of haplotypes (H), number of polymorphic sites (S), haplotype diversity (H_D) and nucleotide diversity (π). In order to visualize the geographic distribution of mtDNA genetic diversity, we also performed a spatial interpolation of population H_D and π values as described for microsatellite makers.

2.4. Genetic structure analyses

For the microsatellite dataset, we inferred genetic structure using Bayesian clustering analyses in Structure 2.3.3 (Pritchard et al., 2000; Falush et al., 2003a). We considered correlated allele frequencies and an admixture model without prior information on population origin. We performed 10 independent runs for each value of $K = 1$ –25 with a burn-in period of 2×10^5 steps and a run length of 1×10^6 Markov chain Monte Carlo (MCMC) cycles. The number of populations best fitting the dataset was defined using log probabilities $[\text{Pr}(X|K)]$ (Pritchard et al., 2000) and the ΔK method (Evanno et al., 2005). We used the Greedy algorithm in the program CLUMPP 1.1.2 (Jakobsson and Rosenberg, 2007) to align replicated runs and average individual assignment probabilities for the most likely K values. Afterwards, we produced bar plots displaying probabilities of individual membership using DISTRUCT 1.1 (Rosenberg, 2004). Complementarily, we visualized genetic differentiation among Structure clusters for the most likely K values by constructing a neighbor-joining (NJ) tree based on net nucleotide distances (Pritchard et al., 2010) using NEIGHBOR program as implemented in PHYLIP 3.695 software (Felsenstein, 2013). Net nucleotide distances represent the average amount of pairwise difference between alleles from different populations (for more details see, Pritchard et al., 2010). This distance has been described as suitable for drawing trees to show the differentiation among clusters inferred by Structure (e.g. Falush et al., 2003b).

For mtDNA, we assessed population genetic structure using a spatial analysis of molecular variance as implemented by SAMOVA 2.0 (Dupanloup et al., 2002). This method employs a simulated annealing procedure to identify the optimal grouping option (K) for the data by

maximizing the among-group component (F_{CT}) of the overall genetic variance. We conducted 10 independent runs for each value of $K = 1$ –12, using default parameters and 500 simulated annealing processes. Mean F_{CT} values and their standard deviation were plotted to determine the most likely population clustering solution (Dupanloup et al., 2002). We only included in this analysis those populations with ≥ 4 sequenced individuals for COI.

We visualized spatial patterns of nuclear and mtDNA genetic structure by interpolating probabilities of population membership to each inferred genetic cluster from Structure and SAMOVA analyses using the ‘maps’ function from ‘POPSutilities’ (Jay et al., 2012; François, 2016) in R 3.2.3 (R Core Team, 2015).

2.5. Phylogenetic analyses and divergence times

We employed BEAST 1.8.0 (Drummond et al., 2012) to obtain a combined estimation of an ultrametric phylogenetic tree and divergence times using sequence data for the COI gene fragment. Analyses were conducted applying a HKY + I model of sequence evolution, which was selected as the best-fitting nucleotide substitution model for our dataset via the Bayesian Information Criteria (BIC) as implemented in jModelTest2 (Darriba et al., 2012). We assumed a normal distributed substitution rate of 0.0169 (± 0.0019 SD) per site per million years for COI gene ($\sim 1.69\%$ per million year divergence rate; Papadopoulou et al., 2010). We ran several analyses considering different clocks and demographic models (Table S2). The best-fitting clock and demographic model to our dataset was determined via Akaike’s information criterion (AIC) through Markov chain Monte Carlo (AICM; Baele et al., 2012) with 100 bootstraps in Tracer 1.5 software. Each analysis was run with two independent MCMC chains of 100 million generations (sampling every 10,000 generations and discarding the first 10% as burn-in) and we used Tracer to examine stationarity and convergence of the chains and confirm that effective sampling sizes (ESS) for all parameters were > 200 . We used LogCombiner 1.8.0 to discard 10% of trees as burn-in and combine tree files from replicated runs. We used TreeAnnotator 1.8.0 to obtain maximum credibility trees and FigTree 1.4.2 to visualize final trees. Complementarily, we used PopART software (Leigh and Bryant, 2015) to produce a statistical parsimony network and infer the phylogenetic relationships among COI haplotypes.

2.6. Demographic analyses

We inferred past demographic changes for the main COI clades using three different approaches. First, we calculated Fu’s F_s (Fu, 1997), Tajima’s D (Tajima, 1989) and R_2 statistics (Ramos-Onsins and Rozas, 2002) and tested their significance by generating 10,000 coalescent simulations in DnaSP software. For neutrally evolving loci, significant and negative (F_s and D) or positive (R_2) deviations of these indexes from zero are interpreted as past population expansions. Second, for each lineage we calculated mismatch distributions of pairwise nucleotide differences (Rogers and Harpending, 1992) under the sudden expansion model by 1000 bootstrap replicates using Arlequin. The goodness-of-fit between observed and expected distributions was tested by calculating sum of squared deviations (SSD; Schneider and Excoffier, 1999) and Harpending’s Raggedness index (H_{rg} ; Harpending, 1994) in Arlequin. A unimodal mismatch distribution and small and non-significant SSD and H_{rg} indexes are indicative of demographic expansions. Finally, we inferred changes in effective population sizes (N_e) over time for each lineage using the coalescent-based Bayesian skyline method (BSP) (Drummond et al., 2005) as implemented in BEAST 1.8.0. We used a piecewise constant skyline model and a number of 10 groups for every lineage (only five groups were considered for northwestern, central and southern France, NWCSF, lineage due to its small sample size) (Ho and Shapiro, 2011). Time and population size were calibrated assuming a strict clock prior (as supported by exploratory runs) and the substitution rate was the same considered for phylogenetic analyses. The best-

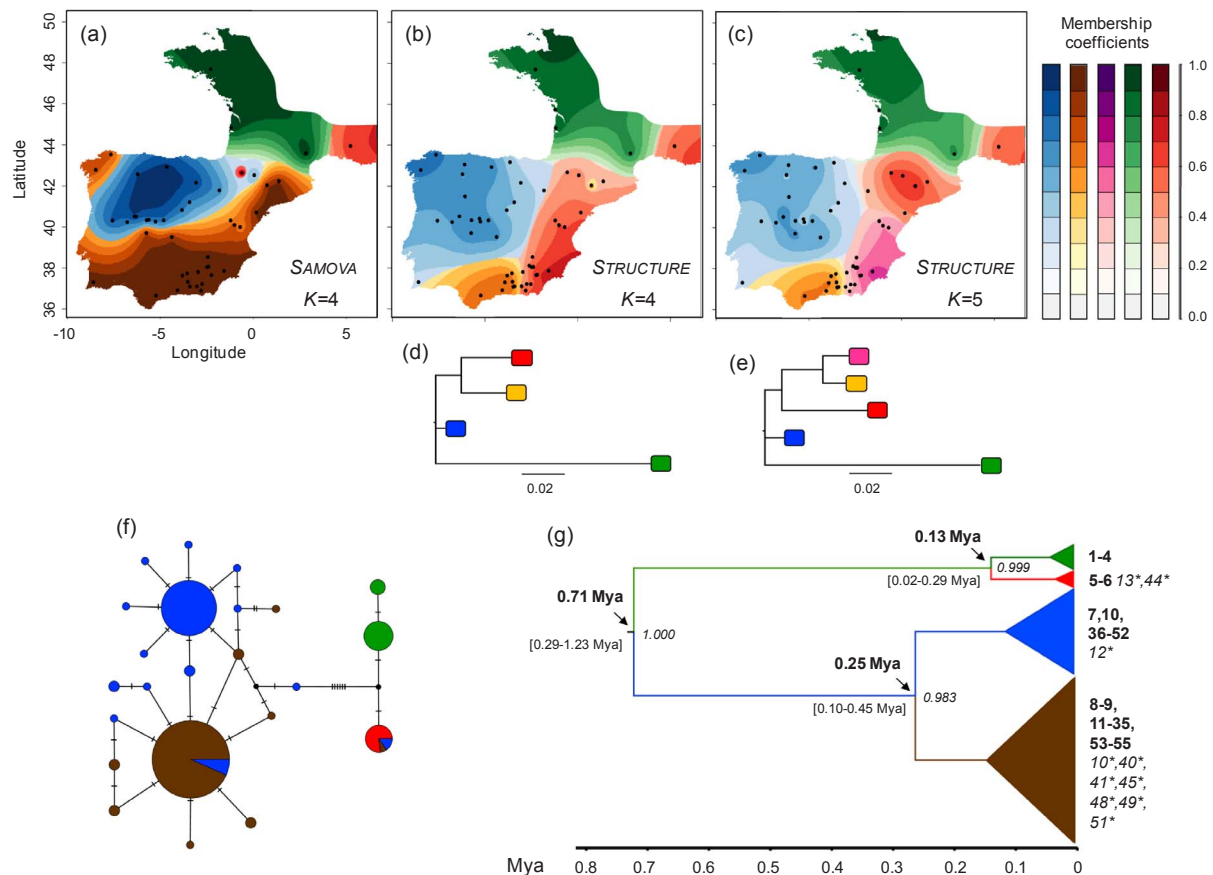


Fig. 1. Results of clustering and phylogenetic analyses for the scrub-legume grasshopper across its distribution range. The top panels represent the geographic distribution of the genetic groups inferred by (a) SAMOVA for mitochondrial cytochrome oxidase subunit I (COI) gene fragment and (b, c) by structure for nuclear microsatellite markers. In these maps, increasingly darker colours indicate higher membership coefficients to a given genetic group. Black dots in the maps indicate the location of sampling sites. Panels (d, e) show neighbor-joining trees based on net nucleotide distances among genetic clusters inferred by Structure for $K = 4$ and $K = 5$, respectively. Colour codes in these neighbor-joining trees correspond to those from the genetic clusters displayed in maps from panels (b, c). Branch lengths in the trees displayed in panels (d, e) show the differentiation among genetic clusters in terms of their net nucleotide distances, which is defined as the average amount of pairwise difference between microsatellite alleles from different populations. Panel (f) shows a statistical parsimony network inferred from COI haplotypes. Colour codes represent the geographic distribution of the four genetic groups inferred by SAMOVA and shown in panel (a). Circle size is proportional to the relative frequency of a given haplotype. Some haplotypes are presented in different geographic regions. Panel (g) represents a maximum clade credibility tree for COI with estimated ages of divergence (mean and lower and upper 95% highest posterior density) for each main node. Bayesian posterior probability for each main clade is indicated at the right of the node. Tip labels in bold type indicate the code of the populations represented in each collapsed clade. Populations codes in italics and with an asterisk indicate those populations assigned primarily to another phylogroup but that present some individuals in that phylogroup. Colour codes represent the four different phylogroups whose geographic distribution is in accordance with the four genetic groups inferred by SAMOVA (panel a). Population codes are described in Table S1. (For interpretation of the references to colour in this figure legend, the reader is referred to the web version of this article.)

fitting nucleotide substitution model for each dataset (i.e. lineage) was determined using jModelTest2 (Table S3). Number of independent replicates for each dataset, MCMC chains lengths and examination of stationarity, convergence and ESS values was conducted as described in the previous Section 2.5.

2.7. Testing demographic scenarios: Approximate Bayesian Computation (ABC)

We used an Approximate Bayesian Computation (ABC) framework to compare different plausible scenarios of population divergence and past demography in the scrub-legume grasshopper (Beaumont, 2010). The topology of the different tested scenarios was designed and informed with phylogenetic and clustering analyses (Figs. 1 and 2). We considered different scenarios of population bottlenecks that were designed on the basis of observed spatial patterns of genetic diversity and climate niche distribution models for the scrub-legume grasshopper and its host-plant species (see next Section 3) (Figs. 2 and 3, Fig. S3). We defined five main population groups by pooling sampling sites according to their geographic location and the results obtained from phylogenetic and clustering analyses (e.g. Inoue et al., 2015; Tsuda

et al., 2015). Our five population groups were northwestern, central and southern France (NWCSF), eastern France and Pyrenees (EF), northern Iberia (NI), eastern Iberia (EI) and southern Iberia (SI) (see Figs. 1c and 2). Given that these population groups highly differed in the number of available samples, we randomly selected a subset of 40 individuals per group ($n = 200$) (for a similar approach, see Shaw et al., 2015). Individuals were selected aiming to maximize the number of samples with available mtDNA sequence data and minimize missing data for microsatellite markers. This approach also allowed us to reduce the computational demands and test a high number of plausible evolutionary and demographic scenarios (see also Tsuda et al., 2015). The first scenario (scenario 1), considered as null model, consisted of a simultaneous split of all these five groups. The second scenario (scenario 2) predicts an old split between an ancestral French clade and the ancestral Iberian one. Afterwards, Iberian populations (NI, EI and SI) diverged simultaneously from each other, and French populations split originating the NWCSF and EF groups. The third scenario (scenario 3) is similar to the second one, but predicts a hierarchical divergence of the Iberia groups at two different times: an older split of NI populations from the rest of the Iberian groups followed by a more recent split of EI and SI populations (see Fig. 2). Because of genetic diversity estimates

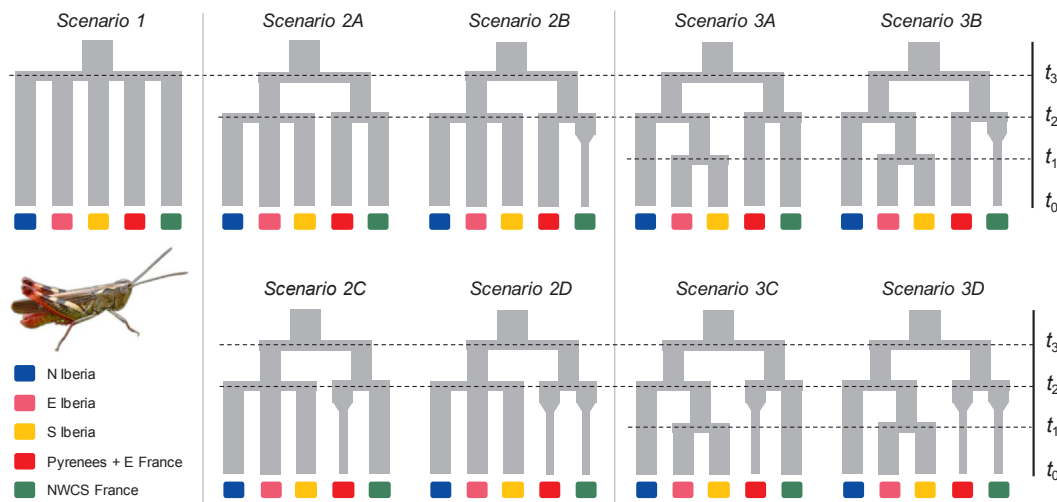


Fig. 2. Different scenarios of population divergence and past demography for the scrub-legume grasshopper compared using an Approximate Bayesian Computation (ABC) approach ($t\#$ represents time in number of generations). Population groups were defined as northern Iberia (blue), eastern Iberia (pink), southern Iberia (yellow), eastern France and Pyrenees (red) and northwestern, central and southern France (green) according to their geographic distribution and the results from clustering analyses. Colours of these genetic groups are in accordance to the genetic clusters inferred by Structure for $K = 5$ (see Fig. 1c, e). (For interpretation of the references to colour in this figure legend, the reader is referred to the web version of this article.)

for French and Pyrenean populations were consistently lower than those obtained for Iberian ones, we considered four different demographic hypotheses for scenarios 2 and 3: (A) no change in effective population sizes, considered as the null demographic model, (B) a population bottleneck in the NWCSF group, (C) a population bottleneck

in the EF group, and (D) population bottlenecks in both NWCSF and EF groups (see Fig. 2). Bottlenecks were considered as a permanent reduction in effective population size (i.e. with no subsequent demographic expansion) based on the results from ecological niche models, which predicted overall low climatic/habitat suitability throughout

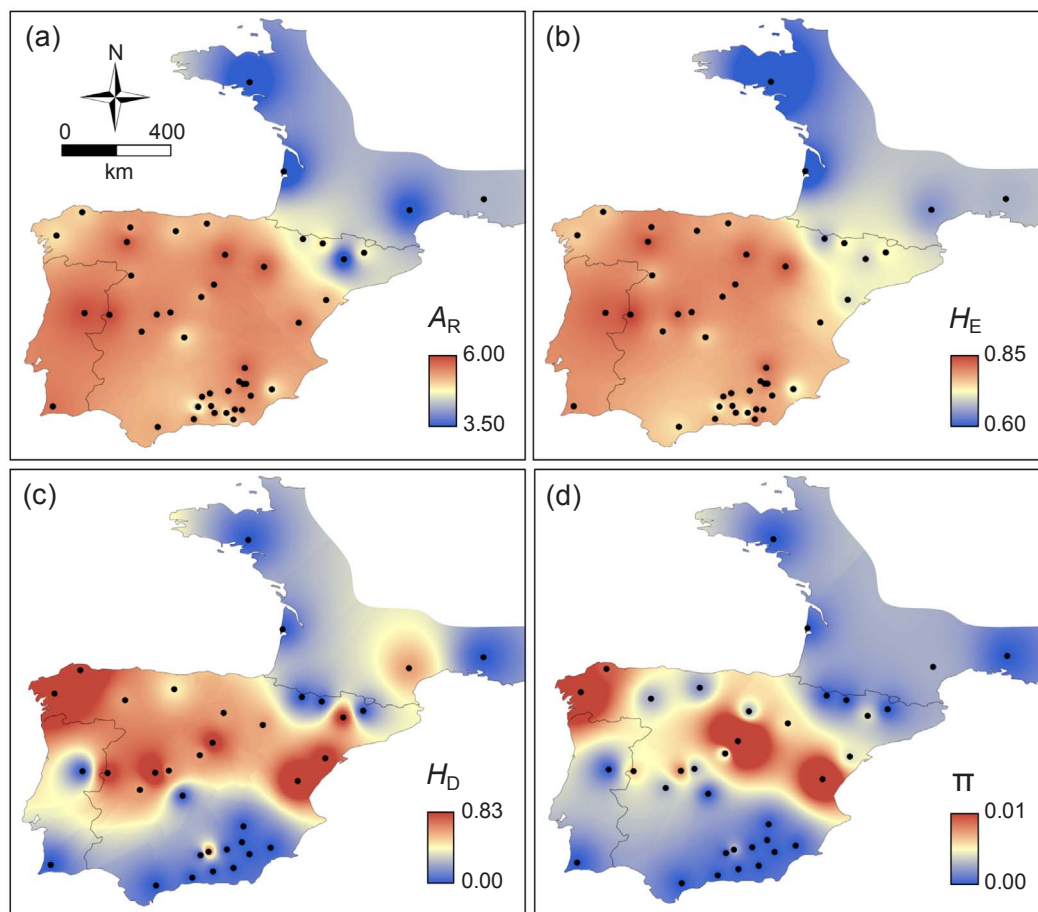


Fig. 3. Maps displaying spatial patterns of genetic diversity at nuclear (A_R , allelic richness, panel (a); H_E , expected heterozygosity, panel (b)) and mtDNA (H_D , haplotype diversity, panel (c); and π , nucleotide diversity, panel (d)) markers across the distribution range of the scrub legume grasshopper. Black dots indicate the location of sampling sites.

France and the Pyrenees during the last 21,000 years (see Section 3.5).

We conducted all the computations in DIYABC 2.0.4 combining nuclear and mitochondrial markers (Cornuet et al., 2014). We ran one million of simulated datasets per scenario assuming a 1:1 female to male sex ratio. We used a generalized mutation model (GSM) and no single nucleotide indels for the microsatellite data and a HKY model of sequence evolution for COI. Summary statistics (SS) for microsatellite markers and mtDNA marker are detailed in Table S4. Pre-evaluation of results based on Principal Components Analyses (PCA) as implemented in DIYABC showed that the cloud of simulated SS were not enough close to our observed SS for any competing scenario. Following the approach by Fontaine et al. (2013) (see also Andersen et al., 2017; Noguerales et al., 2017), we solved this issue by discarding those microsatellites markers with the highest frequency of null alleles, estimated using the Expectation Maximization (EM) algorithm implemented in the program FreeNA (Chapuis and Estoup, 2007). Accordingly, we retained a subset of seven microsatellite markers for all ABC analyses (Noguerales et al., 2017). Information from previous studies (Noguerales et al., 2017) and a pre-evaluation of scenarios and prior distributions were employed to adjust the priors of effective population sizes (N_e) and timing of divergence (t) to their most appropriate values (see Table S4), assuming a uniform prior probability distribution for them. This procedure was also performed to evaluate different magnitudes of reduction in effective population sizes (10, 25, 50, 75, 90%) in population groups for which we hypothesized to have experienced a demographic bottleneck. Following this procedure, prior values of N_e for groups with an assumed population bottleneck was set to 10–500,000 individuals, which was 50% smaller than N_e priors for groups with constant population sizes (i.e. no bottleneck assumed). Selection of the most probable scenario, confidence in scenario choice (type I and type II errors), model checking and estimation of the posterior distribution of all parameters under the best supported model were performed as detailed in Ortego et al. (2015b).

2.8. Ecological niche modelling

We modeled the potential distribution of the scrub-legume grasshopper to assess whether habitat suitability and stability shape its geographic patterns of genetic diversity. We reconstructed the present and past distribution of the scrub-legume grasshopper considering four different subsets of environmental layers: (i) all bioclimatic layers available in WorldClim (Hijmans et al., 2005); (ii) all bioclimatic layers plus a layer of host-plant species richness obtained from climate niche models built for each host-plant species (see below); (iii) only the single most-explicative bioclimatic layer and host-plant species richness; and (iv) only the layer of host-plant species richness.

We employed the maximum entropy presence-only algorithm implemented in Maxent 3.3.3 (Phillips et al., 2006; Phillips and Dudik, 2008) to build species-specific ecological niche models (ENMs) for each host-plant species using the 19 bioclimatic variables available in WorldClim at 30 arc-sec resolution (Hijmans et al., 2005). It has been demonstrated that overparameterized models could perform better than underparameterized ones and thus we initially included all 19 bioclimatic variables in Maxent model building (Warren and Seifert, 2011; Freeman and Mason, 2015). Maximum iterations were set to 5 000 to ensure model convergence. Models for the different host-plants were built using occurrence data available in the Global Biodiversity Information Facility (GBIF; Table S5). All records were spatially checked to exclude species misidentifications, geo-referencing errors and duplicate locations that fell into the same map pixel. Records in areas where the different species are considered non-native based on the literature were also discarded (Talavera et al., 2001; Anthos, 2016). We limited the geographic extent of the climate layers to an area approximately 20% larger than the known distribution range of each host-plant species following suggestions from Anderson and Raza (2010). Model performance was assessed using the area under the receiver

operating characteristic curve (AUC) estimated from test data after averaging over 10 cross-validation replicate runs. To obtain the distribution of the species during the Last Glacial Maximum (LGM, c. 21,000 BP), we projected contemporary species-climate relationships to the LGM using the Community Climate System Model (CCSM3; Collins et al., 2006) from the Paleoclimate Modelling Intercomparison Project Phase II (PMIP2; Braconnot et al., 2007). Layers for the LGM were downloaded from WorldClim at 2.5 arc-min and interpolated to 30 arc-sec resolution. The “fade by clamping” option in Maxent was applied to the past predictions in order to reduce unreliable extrapolation onto extensive areas with environmental conditions not encountered during model training (Phillips et al., 2006). In order to obtain a proxy of overall host-plant species richness and summarize climate niche models of all host-plant species, we converted logistic output maps into binary maps (presence = 1; absence = 0) using threshold values for occurrence based on the maximum training sensitivity plus specificity (MTSS) obtained for each host-plant species (Liu et al., 2005). Afterwards, we summed all binary maps of the thirteen host-plant species separately for current and LGM periods.

For the scrub-legume grasshopper, the four subsets of models described above were built using a total of 287 occurrence locations obtained from our own sampling, the GBIF database, and the literature (Llucà-Pomares, 2002; Defaut, 2011). Niche models were built and projections were performed as described above for host-plants. We assessed the relative support of each Maxent model using the sample-size adjusted Akaike’s information criterion (AIC_c) calculated as implemented in ENMTools (Warren et al., 2010).

We considered that a grid cell was ‘stable’ when it presented suitability scores above the MTSS threshold for both the present and the LGM periods (for a similar approach see Wachter et al., 2016). Afterwards, stability maps for each Maxent model of the scrub-legume grasshopper were generated by averaging current and LGM suitability maps that included only ‘stable’ pixels across both periods (all other pixels were considered to have stability = 0). Finally, we used ArcGIS 10.3 and a buffer of 10 km² around sampling locations to extract values of climate/habitat suitability stability for each studied population and the models based on (i) all bioclimatic variables (C_{STA}), (ii) all bioclimatic variables and host-plant species richness ($C-HP_{STA}$), (iii) only the single most-explicative bioclimatic variable and host-plant species richness (C^*-HP_{STA}), and (iv) only host-plant species richness (HP_{STA}). All raster calculations were conducted using Raster package (Hijmans and van Etten, 2016) in R.

2.9. Genetic diversity and estimates of habitat stability

We tested the hypothesis that population genetic diversity in the scrub-legume grasshopper is correlated with stability of habitat suitability defined by climatic tolerances of the focal species and/or distributional shifts of its host-plants during the last 21,000 years. In particular, we tested the association between nuclear (A_R , H_E) and mtDNA (H_D and π) genetic diversity estimates and stability of climate/habitat suitability for the scrub-legume grasshopper obtained from the four different Maxent models described in the previous Section 2.8. To this end, we used generalized linear models (GLMs) and an information-theoretic model selection approach (Burnham and Anderson, 2002). GLMs were constructed considering a Gaussian error distribution and an identity link function using R package lme4 (Bates et al., 2015). Longitude and latitude were included as covariates to take in account possible geographical clines of genetic diversity (Guo, 2012; Eckert et al., 2008). GLMs were fitted considering potential bias resulted from model overfitting and spurious relationships between dependent and independent variables because of the high collinearity between the different estimates of climate stability (Burnham and Anderson, 2002; Arnold, 2010). Accordingly, we constructed the different combinations of GLMs only including one of the estimates of climate stability at a time. Given that the precision of genetic diversity estimates may differ

among populations due to differences in sample sizes, we used a weighted least square (WLS) method where weight equals the sample size for each studied population. We analyzed the goodness of fit of the models using AIC_C values (Burnham and Anderson, 2002; e.g. Noguerales et al., 2015). We ranked models according to their AIC_C values using the R package MuMIn (Barton, 2015) and those models with $\Delta AIC_C \leq 2$ were considered to have similar empirical support than the best model (i.e. that with the lowest AIC_C ; Burnham and Anderson, 2002). The Akaike weight (ω_i) was calculated for each model, which represents the relative probability that a given model will be the best among those considered. For each best ranked models ($\Delta AIC_C \leq 2$), we calculated separately the 95% confidence intervals (CI) of their estimators. The effect of variables was considered significant if the 95% confidence intervals (CI) of their estimators excluded zero (Burnham and Anderson, 2002). If the null model (i.e. without predictors) was included within the best ranked models ($\Delta AIC_C \leq 2$), we considered that any remaining variables included in other equivalent models ($\Delta AIC_C \leq 2$) did not have a significant effect on the dependent variable.

3. Results

3.1. Spatial patterns of genetic diversity and structure

Nuclear genetic diversity ranged from 3.54 to 5.98 for A_R , and from 0.59 to 0.85 for H_E . Genetic diversity at nuclear markers was spatially homogenous throughout Iberian populations, which exhibited the highest values, whereas French and Pyrenean populations showed the lowest levels of genetic variability (Fig. 3). At mitochondrial level, we recovered 23 different haplotypes but ~50% of the populations exhibited no genetic variation. In populations that showed intra-population genetic variation at mtDNA, genetic diversity estimates ranged from 0.28 to 0.83 for H_D , and from 0.0005 to 0.0108 for π . Populations from east and northwestern Iberia presented the highest levels of mtDNA genetic diversity (Fig. 3).

Structure analyses showed a steadily increase of log probabilities [Ln Pr (X|K)] from $K = 2$ to $K = 5$ (Fig. S1c). According to the ΔK method, the best-supported number of genetic clusters was $K = 4$ (Fig. S1c). When we considered $K = 4$, a first cluster included all the populations located in northwestern France and also the population ‘Col de Fontfroide’ from the Massif Central in southern France (Fig. 1b, Fig. S1d). A second cluster included the easternmost French population (‘Gordes’) and the Pyrenean and eastern Iberian populations. The populations from south Iberia were included in a third cluster and a fourth cluster was primarily composed of populations from central and north Iberia (Fig. 1b, Fig. S1d). The above described clustering pattern was similar when we considered $K = 5$, however the easternmost French population (‘Gordes’) and the Pyrenean populations were included in a new cluster differentiated from eastern Iberian populations (Fig. 1c, Fig. S1d). Neighbor-joining trees considering both grouping solutions revealed that the NWCSF cluster was the most genetically differentiated (Fig. 1d, e). Structure analyses showed that the F -value, which represents the amount of drift for each cluster from a common ancestral population, was 0.24 for the NWCSF cluster whereas this index ranged from 0.04 to 0.06 in the remaining genetic clusters.

SAMOVA analyses on mtDNA showed that mean F_{CT} values increased from $K = 2$ to $K = 5$, and reached a plateau for $K = 7$ (Fig. S1b). The clustering solution for $K = 4$ was consistent with the main four main clades inferred by phylogenetic analyses (see next Section 3.2). The first cluster grouped the populations from northwestern France and the population ‘Col de Fontfroide’ from southern France. A second group was composed of the easternmost French (‘Gordes’) and westernmost Pyrenean (‘Borau’) populations. The east, south-central and northwestern Iberian populations composed a third group. Finally, north-central Iberian populations were included in the fourth cluster (Fig. 1a, Table S1). Clustering solutions for $K = 5$ –7 yielded additional genetic groups that were exclusively composed by a single population:

‘Puerto de la Quesera’ (Central Iberia), ‘Buerba’ (Western Pyrenees) and ‘Sierra del Toro’ (Eastern Iberia). These additional clusters were not congruent with network or phylogenetic analyses (Fig. 1f, g) and, for these reasons, $K = 4$ was considered as the clustering scheme that best explained the spatial genetic structure of the species at a range-wide scale.

3.2. Phylogenetic analyses and divergence times

Phylogenetic reconstruction in BEAST was conducted using a strict clock and a constant demographic model, the one that best fitted our data according to the model selection procedure implemented in Tracer (Table S2). The phylogenetic tree revealed four well-supported phylogroups, which were equivalent to those inferred by SAMOVA (Fig. 1g). Most individuals from the same population were grouped in a single phylo-group. However, Iberian phylo-groups were not reciprocally monophyletic and exhibited certain degree of admixture (i.e. populations presented individuals assigned to different clades) (Fig. 1g). Divergence times indicated a split of French and Iberian populations around the Mid Pleistocene (~0.71 Mya), whereas divergence within Iberian and French clades took place more recently, around the Late Pleistocene (~0.25 and ~0.13 Mya, respectively) (Fig. 1g). Nevertheless, divergence times must be considered cautiously given that their respective confidence intervals are broad (Fig. 1g). Similar to the phylogenetic reconstruction in BEAST, network genealogy revealed that the 23 different haplotypes recovered clustered in four main groups exhibiting a highly congruent geographical distribution (Fig. 1f).

3.3. Demographic analyses

Northern and south/southeastern Iberia lineages presented significant negative F_u 's F_s and Tajima's D and significant positive R_2 statistics, which could be interpreted as past population expansions (Table S3). All tests for F_u 's F_s , Tajima's D and R_2 statistics failed to reject the null hypothesis of constant population size for the French lineages (Table S3). Pairwise mismatch distributions were unimodal although skewed to the lowest pairwise nucleotides differences estimates for all lineages. Test of goodness-of-fit between observed and expected distributions were not significant, which would suggest that all lineages have undergone demographic expansions (in all cases for SSD and H_{rg} , P -values > 0.16) (Fig. S2). Finally, BSP analyses showed a more complex demographic history and suggested that northern and southern/eastern Iberia lineages experienced a demographic expansion that began around 20,000 years ago followed by a subtle negative trend in N_e during the most recent time interval (Fig. S2). Conversely, skyline plots for NWCSF and all lineages from France and the Pyrenees revealed that their effective population sizes have remained steadily small during the last 50,000 years (Fig. S2). However, it should be noted that these demographic inferences presented very large 95% highest posterior densities (HPD) values of N_e for all lineages and must be interpreted with caution (Fig. S2).

3.4. Testing demographic scenarios: Approximate Bayesian Computation (ABC)

ABC analyses indicated that “scenario 3B” of population divergence and past demography had the highest posterior probability and its 95% confidence intervals did not overlap with those obtained for other scenarios (Table 1). This scenario was defined by a population bottleneck for the NWCSF group and a hierarchical divergence scheme for the Iberian groups. For the best-supported scenario, we found that observed data fell within simulated data and all SS used for model checking showed P -values > 0.2, suggesting good model fit. Overall type I and type II errors were relatively low (< 0.25, Table 1) and RMAEs exhibited values lower than 0.25 in most parameters, indicating a good reliability of their estimates (Table 2). Assuming a constant mutation

Table 1

Posterior probability for each of the nine tested scenarios of population divergence and past demography in the scrub-legume grasshopper and 95% confidence intervals (CI) based on the weighted polychotomous logistic regression approach for approximate Bayesian Computation Analyses (ABC). Type I and II errors for the best supported scenario (in bold) are indicated.

Scenario	Posterior probability	95% CI	Type I error	Type II error
1	0.0179	[0.0153–0.0205]		
2A	0.0299	[0.0272–0.0325]		
2B	0.0771	[0.0733–0.0809]		
2C	0.0189	[0.0164–0.0215]		
2D	0.0467	[0.0435–0.0498]		
3A	0.1640	[0.1587–0.1693]		
3B	0.3792	[0.3718–0.3866]	0.246	0.220
3C	0.0828	[0.0792–0.0865]		
3D	0.1835	[0.1777–0.1893]		

Table 2

Posterior parameter estimates (median and 95% confidence intervals) for the best supported scenario of population divergence and past demography (scenario 3B, see Fig. 2). Estimates are based on 1% of simulated datasets closest to the observed values. Relative median absolute errors (RMAE) based on 500 pseudo-observed data sets are also indicated for each parameter.

Parameter	Median	$q_{0.025}$	$q_{0.975}$	RMAE
$N_{NWCSF-B}$	283,000	127,000	459,000	0.230
N_{EF}	767,000	421,000	980,000	0.206
N_{NI}	747,000	428,000	967,000	0.213
N_{EI}	640,000	252,000	969,000	0.232
N_{SI}	682,000	291,000	971,000	0.233
N_F	658,000	212,000	983,000	0.278
N_I	688,000	120,000	984,000	0.403
N_{ESI}	563,000	556,000	978,000	0.352
N_X	465,000	26,700	969,000	0.376
t_1	62,900	6830	279,000	0.408
t_2	230,000	62,300	670,000	0.224
t_3	603,000	188,000	978,000	0.146
μ_{mDNA}	5.46×10^{-6}	2.24×10^{-6}	1.68×10^{-5}	0.392
μ_{mtDNA}	2.12×10^{-9}	1.21×10^{-9}	4.30×10^{-9}	0.269

$N_{NWCSF-B}$, effective population size of the northwestern, central and southern France group (assuming a population bottleneck event).

N_{EF} , effective population size of the eastern France and Pyrenees group.

N_{NI} , effective population size of the northern Iberia group.

N_{EI} , effective population size of the eastern Iberia group.

N_{SI} , effective population size of the southern Iberia group.

N_F , effective population size of the ancestral France group.

N_I , effective population size of the ancestral Iberia group.

N_{ESI} , effective population size of the ancestral south and eastern Iberia group.

N_X , effective population size of the ancestral population.

t_1 , time (in generations = years) to the most recent divergence event.

t_2 , time (in generations = years) to the intermediate divergence event.

t_3 , time (in generations = years) to the most ancient divergence event.

μ_{mDNA} , mean mutation rate for microsatellites markers.

μ_{mtDNA} , mean mutation rate per site per generation for the mitochondrial marker (COI).

rate, the posterior estimates of N_e for the NWCSF group were much lower (median $N_e = 283,000$) than those obtained for the remaining groups (median $N_e = 640,000$ – $767,000$; Table 2). A similar result was obtained when we calculated the posterior parameter estimate for the competing scenario assuming no bottleneck for the NWCSF group (“scenario 3A”; median $N_e = 244,000$), supporting that our estimates of N_e for this group were consistent and not biased by the setting of prior bounds. Considering the one-year generation time of scrub-legume grasshopper (Default, 2011), the French ancestral group was estimated to diverge from the ancestral Iberian group $\sim 600,000$ years ago (t_3). Subsequently, a split within French and Iberian populations took place $\sim 230,000$ years ago (t_2), whereas the most recent divergence happened between the eastern and southern Iberian groups, $\sim 60,000$ years ago (t_1). These estimates of divergence times are highly consistent with

those inferred by phylogenetic reconstruction in BEAST (Fig. 1 g).

3.5. Ecological niche modelling

Species-specific niche models for host-plants generally presented high AUC values (average AUC across species: 0.85; range: 0.621–0.983), indicating overall good model performance (Table S5). Host-plants models showing the lowest AUC values (< 0.75) correspond to taxa widely distributed throughout Europe and North Africa (*C. scoparius*, *G. scorpius* and *U. europaeus*; Table S5). Inspection of current predicted distributions of host-plants confirmed that species-specific niche models yielded distribution patterns coherent with their respective observed distributions.

For the scrub-legume grasshopper, niche models presented AUC values ranging from 0.788 to 0.867 (Table S5). The most supported model (i.e. with the lowest AIC_C) for the scrub-legume grasshopper was the one based on all the nineteen bioclimatic variables (model i; Table S5). In this model, the variable relative to “mean temperature during the driest quarter” (bio9) resulted to be the most important predictor as indicated Maxent’s jackknife analysis (i.e. it provided the highest gain when used in isolation; Table S5). The second most-supported model in terms of AIC_C value (model ii; $\Delta AIC_C = 10.03$) was that including all the bioclimatic variables together with host-plant species richness predictor. In this model, host-plant species richness was the most important predictor (i.e. it provided the highest gain when used in isolation and also decreased the gain the most when it was omitted; Table S5). These two models (i and ii) exhibited the highest model performance in terms of AUC value. Similarly, host-plant species richness resulted to be the most important variable when it was included in a model only with the most-important bioclimatic predictor (bio9) (model iii; Table S5). This model exhibited a lower support ($\Delta AIC_C = 186.26$) in comparison to the models including a higher number of variables (Table S5). Finally, the model including only host-plant species richness (model iv) yielded the lowest performance and the lowest support ($\Delta AIC_C = 336.05$) (Table S5).

According to the best-supported model (model i), the current distribution of the scrub-legume grasshopper is strongly fragmented and restricted to the main Iberian and French mountain ranges, northwestern Iberia, and the Atlantic French coast (Fig. S3a). Projections into the LGM indicated that the distribution of the scrub-legume grasshopper was more widespread and its populations exhibited higher connectivity during this period than in the present, particularly in the Iberia Peninsula (Fig. S3b). We observed that most sampling locations were located in regions with high climate suitability stability (Fig. S3c). Nonetheless, populations from France and the Pyrenees were located in areas characterized by low climate suitability both in the present and during the LGM (Fig. S3c).

The model including host-plant species richness and all bioclimatic layers (model ii, $\Delta AIC_C = 10.03$; Table S5), exhibited a present-day distribution similar to that predicted by the best ranked model (Fig. S3a, d). These two models presented subtle differences in their past predicted distributions: model (ii) predicted areas with lower suitability in western Iberian as well as higher suitability in western France during the LGM compared to model (i) including only bioclimatic variables (Fig. S3b, e). Similarly to the best-supported model, model (ii) showed that most populations are located on relatively large areas of high habitat suitability stability, with the exception of those from western and eastern France (Fig. S3f).

The models with lowest support (models iii and iv) wrongly predicted very large present-day suitable areas in western, central and eastern France, while failed to predict high suitability in areas of western and northern Iberia where scrub-legume grasshopper is largely distributed based on current observed occurrences (Fig. S3g, j). Consequently, their projections into the LGM and stability maps showed important differences compared to those obtained from the best ranked models and predicted a more fragmented distribution of the species in

Table 3

Generalized linear models (GLMs) for nuclear genetic diversity of scrub-legume grasshopper (A_R , allelic richness standardized for sample size; H_E , expected heterozygosity) testing the effects of (i) stability of climate suitability (C_{STA}) based on a Maxent model built using all climatic variables, (ii) stability of habitat suitability ($C-HP_{STA}$) based on a Maxent model built using all climatic variables and host-plant species richness, (iii) stability of habitat suitability (C^*-HP_{STA}) based on a Maxent model built using only the most-explicative climatic layer (bio9) and host-plant species richness, and (iv) stability of habitat suitability (HP_{STA}) based on a Maxent model built using only host-plant species richness. Latitude (Lat) and longitude (Lon) were also included as covariates in the models. For each model we indicate AIC_C , sample-size adjusted Akaike's information criterion (AIC) value. We only show best ranked equivalent models ($\Delta AIC_C \leq 2$; for model selection results, see Table S6), for which the 95% confidence intervals (CI) of their estimators were separately calculated. Predictors excluding the value 0 in their 95% CI are indicated in bold type and their effects were considered significant. The predictors HP_{STA} and C^*-HP_{STA} were not included in any of the best ranked equivalent models for nuclear genetic diversity ($\Delta AIC_C \leq 2$; for model selection results, see Table S6).

Models	Predictors	Estimate \pm SE	Lower 95% CI	Upper 95% CI	AIC_C
A_R	Lat	-0.0633 \pm 0.0260	-0.1143	-0.0123	61.20
	Lon	-0.0633 \pm 0.0250	-0.1124	-0.0141	
	C_{STA}	0.6973 \pm 0.2497	0.2077	1.1868	
H_E	Lat	-0.0052 \pm 0.0023	-0.0099	-0.0006	-158.60
	Lon	-0.0060 \pm 0.0022	-0.0105	-0.0015	
	C_{STA}	0.0689 \pm 0.0228	0.0241	0.1138	
H_E	Lat	-0.0045 \pm 0.0026	-0.0096	0.0005	-156.80
	Lon	-0.0070 \pm 0.0023	-0.0115	-0.0024	
	$C-HP_{STA}$	0.0651 \pm 0.0244	0.0172	0.1130	

the Iberia Peninsula during the LGM, particularly when host-plant species richness was the only predictor included in the model (Fig. S3h, k, l, i).

3.6. Genetic diversity and estimates of habitat stability

Model selection for nuclear genetic diversity indicated that latitude, longitude and C_{STA} had a significant effect on A_R (i.e. 95% CIs of such predictors did not cross zero). Similarly, we found that latitude, longitude, C_{STA} and also $C-HP_{STA}$ had a significant effect on H_E (Table 3, Table S6). Latitude and longitude were negatively associated with A_R and H_E , whereas C_{STA} and $C-HP_{STA}$ had a positive effect on genetic diversity estimates (Fig. 4). Model selection for mitochondrial genetic diversity showed that the null model was among the best ranked models ($\Delta AIC_C \leq 2$) for both H_D and π , indicating that no predictor had a significant effect (Table S6).

4. Discussion

Integrating nuclear and mitochondrial markers with a suite of analytical approaches (including phylogenetic Bayesian reconstructions, ecological niche modelling and explicit hypothesis testing using an ABC framework), allowed us to conclude that the scrub-legume grasshopper presents a striking phylogeographic structure resulted from long-term isolation in Iberian and French refugia during Pleistocene glacial cycles. The variability through time of habitat suitability impacted the demographic history of the northernmost populations of the species, a process that reduced local/regional levels of genetic diversity and left detectable signatures of population bottlenecks. Our analyses also support that such process of genetic erosion was explained by habitat suitability stability defined by climate and the spatial distribution of host-plant species richness, indicating the importance of integrating both biotic and abiotic factors into the study of the demographic history of specialist taxa with narrow ecological requirements.

4.1. Past distribution and spatial genetic structure

Analyses of mtDNA showed that populations of the scrub-legume grasshopper split into two major phylogeographic lineages from France and Iberia that probably diverged during the Mid-Pleistocene, around 700,000 years ago. The long branches defining French and Iberian clades in the phylogenetic tree and their geographic coherence suggest a scenario of allopatric divergence that was probably mediated by geographic barriers (i.e. the Pyrenees) and long-term lineage persistence in different refugia (Cooper and Hewitt, 1993; Cooper et al., 1995). This result contrasts with phylogeographic patterns observed for

many temperate-adapted taxa whose present-day northern populations are the result of post-glacial recolonizations from southern Mediterranean peninsulas (Iberian, Italian and Balkan) during warming periods (Taberlet et al., 1998; Schmitt, 2007). The most recent divergence event within Iberian and French lineages probably took place around the Late Pleistocene (c. 250,000 and 130,000 years ago, respectively) and could have been also promoted by isolation in local refugia during interglacial periods (Petit et al., 1999; Snyder, 2016). Thus, the global phylogeographic structure of the species seems to have been mostly driven by the presence of major geographic barriers and temporal changes in the spatial distribution of suitable habitats mediated by Pleistocene glacial cycles. Assuming niche conservatism (Peterson et al., 1999; Noguerales-Bravo, 2009), our best-supported ENM suggests that during interglacials the populations of scrub-legume grasshopper were likely pushed up to higher elevations in response to uphill distributional shifts of its cold-adapted host-plants species, which may be responsible of more recent population fragmentation at local/regional scales (Noguerales et al., 2017). Accordingly, Structure analyses showed a finer genetic structure at regional scales that divided the mitochondrial lineage from east and south Iberia into two different genetic clusters. ABC analyses suggest that these genetic clusters diverged from a common ancestor after the Last Interglacial, likely during a period defined by short warming pulses that took place during the Late Pleistocene (Petit et al., 1999). Overall, the combined effect of the complex topography of the Iberian Peninsula and climate-driven distributional shifts of host-plants could have acted together to reduce or disrupt gene flow among populations of scrub-legume grasshopper at a regional scale (Noguerales et al., 2017).

The observed pattern of multiple refugia throughout the current distribution range of the species has been also documented in many other plants and animals in southwestern Europe and is in good agreement with the "refugia-within-refugia" concept (Gómez and Lunt, 2007; Abellán and Svenning, 2014). Strong genetic subdivision promoted by population isolation in different Pleistocene Iberian refugia has also been reported for the meadow grasshopper (*Pseudochorthippus parallelus*) (Hewitt, 1996; Cooper and Hewitt, 1993). However, contrary to the general pattern of population isolation in northern Mediterranean peninsulas, the existence of a French lineage distributed from the Atlantic coast to Massif Central suggests long-term persistence of our study species outside of the Iberian Peninsula in a cryptic northern refugium (Provan and Bennett, 2008; Stewart et al., 2010; Salvi et al., 2013). The existence of a single and large refugium encompassing from Massif Central to Brittany seems unlikely according to our climatic reconstructions and different hypotheses could explain the origin and the demography of the NWCSF lineage (Schmitt and Varga, 2012). The fact that our study species feeds on several montane or cool-adapted

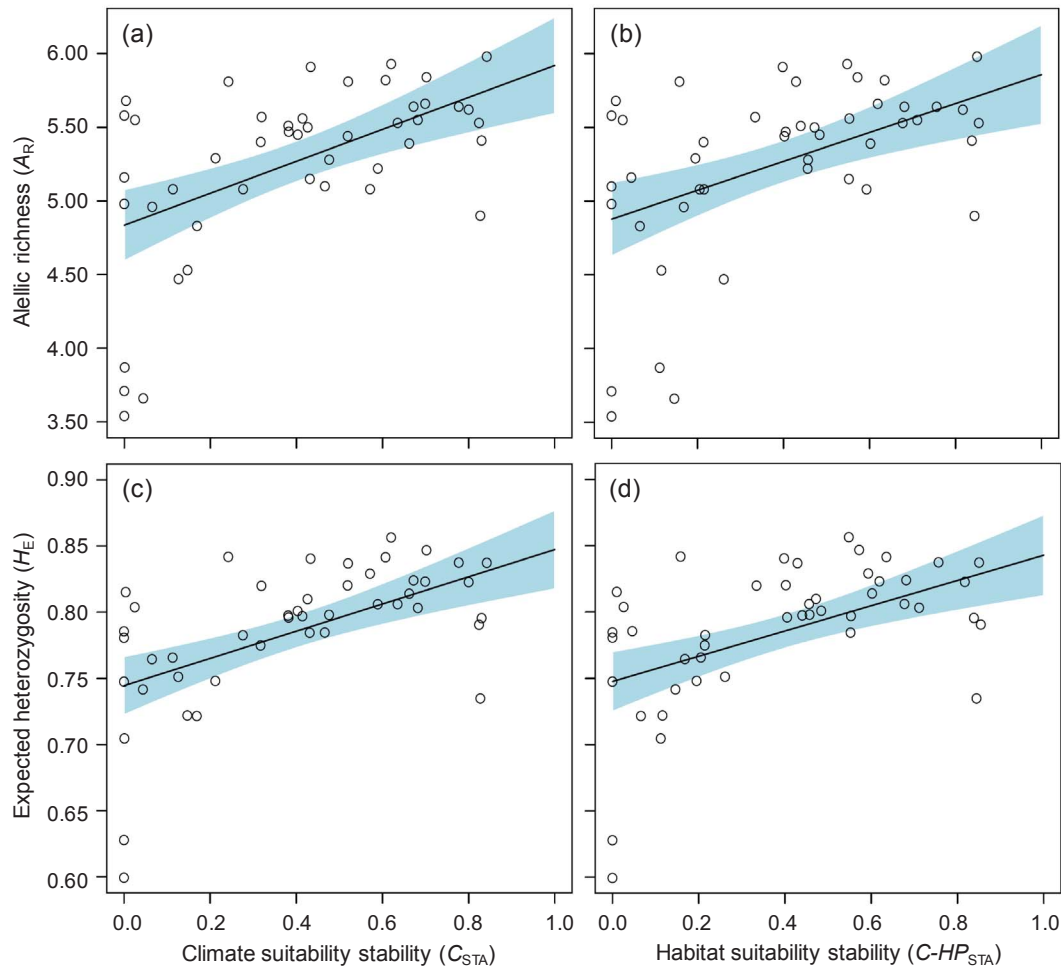


Fig. 4. Scatterplots representing the relationship between (a, b) allelic richness (A_R) and (c, d) expected heterozygosity (H_E) of scrub-legume grasshopper in relation to (a, c) stability of climate suitability (C_{STA}) based on a Maxent model built using all climatic variables and (b, d) stability of habitat suitability ($C-HP_{STA}$) based on a Maxent model built using all climatic variables and host-plant species richness. Regression lines and 95% confidence intervals are shown.

scrub legume species could have facilitated *in situ* population persistence in different micro-refugia during unfavorable periods in the northernmost areas (Parducci et al., 2012). Accordingly, our ENMs suggest a patchy distribution of climatically suitable areas for either the scrub-legume grasshopper or some of its host-plant species since the LGM. Alternatively, the higher mtDNA genetic diversity of populations from Massif Central in south France ('Col de Fontfroide') in comparison with those located along the Atlantic coast may also suggest a recent range expansion from a putative refugium located in this region (Gutiérrez-Rodríguez et al., 2016). As suggested by the best-supported ENM, the more continuous distribution of suitable habitat in the past suggests that scrub-legume grasshopper could have dispersed from the Massif Central to the northwest across central France during favorable periods (Gutiérrez-Rodríguez et al., 2016). This hypothesis is in agreement with the recent idea that the Massif Central was an important reservoir of stable populations and the geographic origin of range expansions for some taxa during the Pleistocene (Schmitt and Varga, 2012; Ursenbacher et al., 2015).

4.2. Habitat stability and species demographic history

The inference of refugia has traditionally relied on species-specific responses to climate (Ashcroft, 2010; Keppel et al., 2012), which are expected to be especially relevant for ectotherm organisms whose niches are often shaped by temperature tolerances (Noguerales et al., 2016b). However, refugium is a broad concept that should be defined

not only taking into account the environmental tolerances and responses of species to climatic oscillations but, ideally, also considering their ecological interactions with other taxa (Ashcroft, 2010; Stewart et al., 2010). The findings from our different analyses revealed an important role of environmental stability on the demographic history of the scrub-legume grasshopper at both population and lineage scales. Demographic reconstructions and ABC analyses supported a population bottleneck in the NWCSF lineage after it split from its sister Pyrenean and Mediterranean French clade, a process that likely resulted in strong genetic drift and erased its levels of genetic variation (Qu et al., 2014). Accordingly, Structure analyses reported that the amount of drift after divergence (F -value) was 0.24 for the NWCSF cluster, whereas all other clusters presented between four- and fivefold lower estimates for this statistic (F -values ranging from 0.04 to 0.06) (for a similar approach see Harter et al., 2004). This, together with the severity of the inferred population bottleneck (N_e of the NWCSF lineage was reduced by ~50% with respect to its ancestral N_e), lend also support to a demographic scenario probably defined by geographically isolated populations inhabiting fragmented patches of suitable habitat that sustain small effective population sizes. In this vein, whereas ecological suitability characterizing the northernmost distribution area of the species make feasible that it has maintained viable populations of scrub-legume grasshopper through time, such populations have probably experienced remarkable demographic fluctuations (i.e. bottlenecks and extinctions-recolonization processes) that ultimately eroded their genetic variability (Yannic et al., 2014; Bidegaray-Batista et al., 2016). In contrast,

our demographic analyses revealed slight signatures of past demographic expansions in the Iberian populations that could have been driven by the higher availability of suitable habitats in the area during the LGM period, as the best-supported ENM suggested. Here, we must note that these analyses should be interpreted with extreme caution due to the overall uncertainty (very large 95% HPD) of our demographic inferences obtained from Bayesian skyline plots (Grant, 2015). In addition, the best-supported ENM indicated that most Iberian populations have been located in environmentally more stable and connected suitable areas during the last 21,000 years, which has probably contributed to maintain larger effective population sizes and higher levels of nuclear genetic variation (Inoue et al., 2015). In this regard, we found a positive association between nuclear genetic diversity (H_E and A_R) and local stability of suitable habitats since the LGM, a result that is in agreement with previous empirical studies addressing the consequences of environmental stability at local/regional scales on the demographic history of different taxa (Qu et al., 2014; Faye et al., 2016; Gutiérrez-Rodríguez et al., 2016). All the foregoing suggest that the spatial trend of genetic diversity is not consequence of serial bottlenecks resulting from northward range expansions as traditionally predicted by the so-called “southern richness vs. northern purity” hypothesis (Hewitt, 2000; Gómez and Lunt, 2007; Canestrelli et al., 2006). In our case, we found evidence that the overall decreasing of neutral genetic diversity with latitude was driven by the different magnitude of demographic fluctuations experienced by long-term persisting populations located in areas showing considerable variation in the impacts of climatic oscillations (Gómez and Lunt, 2007).

Despite the spatial pattern of mitochondrial genetic diversity was partially similar to that inferred from nuclear markers, we did not detect a significant association between estimates of mitochondrial genetic diversity (H_D and π) and stability of climate/habitat suitability. On the one hand, this could be due to the high proportion of populations exhibiting no mitochondrial genetic variability could have weakened the statistical power of our analyses. On the other hand, however, we cannot rule out that the observed signature of mitochondrial genetic variation was primarily shaped by historical factors predating the temporal scale of our estimates of climate/habitat suitability stability.

4.3. Lessons from integrating host-plant interactions into ecological niche models

Although the reliability of the two best-supported ENMs is evidenced by the fact that their resulting climate/habitat suitability stability estimates explained spatial patterns of neutral genetic variation of the focal species, our approach aimed to integrate biotic and abiotic interactions into ENMs may present some uncertainties derived from the usage of host-plant potential distributions that are themselves the product of climate-based ENMs (see also Kuhn et al., 2016). However, this source of error is expected to be minimal as host-plant predicted distributions reflected well their respective contemporary observed distributions. Also, although we are aware that model projections present many inherent caveats (e.g. Hampe, 2004; Nogués-Bravo, 2009; Araújo and Peterson, 2012), our ENM-based approach allowed us to project climate-species relationships into the past and generate layers of host-plant species richness during the LGM, which would have not been feasible only considering present-day raw occurrence data of host-plants (e.g. Freeman and Mason, 2015).

Our ENMs revealed an important contribution of host-plant species richness to explain the distribution of the scrub-legume grasshopper, although the role of this biotic predictor was more patent when it was included in the ENMs in combination with the climatic (abiotic) variables. Although this combined model exhibited the highest model performance in terms of AUC, it was not selected as the best-supported model in terms of ΔAIC_C , likely as a consequence of a penalty because of its higher number of parameters. This model was characterized by

predicting a lower probability of occurrence of the scrub-legume grasshopper in areas where *a priori* its occurrence would be expected due to the presence of suitable climatic conditions according to the species climatic tolerances (Kuhn et al., 2016). Overall, our results are in agreement with other studies stressing the importance of modelling ecological interactions to accurately delineate the potential distribution of species with narrow feeding requirements or involved in host-parasite interactions (Freeman and Mason, 2015; Kuhn et al., 2016).

5. Conclusions

Our study highlights the importance of integrating the potential effects of abiotic (i.e. climate and geography) and biotic components (i.e. inter-specific interactions) into the study of the evolutionary history of specialist taxa with narrow ecological requirements. Harnessing different genetic markers and analytical tools, our integrative approach was able to disentangle numerous cryptic aspects of the demographic trajectories of the scrub legume grasshopper across its entire distribution range. Different lines of evidence pointed to the presence of at least one northern refugium out of the Iberian Peninsula and revealed that the stability of suitable habitats defined by both climate and host-plant species richness had important consequences on the spatial patterns of population genetic variability of the species. Future research combining high-throughput sequencing and spatially-explicit testing of biologically informed models that integrate interspecific interactions could provide a more comprehensive framework to elucidate the factors structuring genetic variation in natural populations (Massatti and Knowles, 2016).

Data accessibility

DNA sequences are deposited in Genbank with accession numbers KY709453-KY709671. The following data are accessible at Mendeley Data repository (doi: <http://dx.doi.org/10.17632/87z7ccgvst.1>): microsatellite genotypes and occurrence records for building Maxent models of *Chorthippus binotatus binotatus* and all its host-plant species.

Authors contributions

VN and JO conceived and designed the study. VN carried out the lab work and analysed the data supervised by JO. VN, PJC and JO collected the samples. VN wrote the manuscript with help of JO and PJC. All authors read and approved the final manuscript.

Conflicts of interest

The authors declare that they have no competing interests.

Acknowledgments

We thank to Conchi Cáliz for her advice during lab genetic work and Bernard Defaut for providing valuable information about sampling locations. Two anonymous referees provided valuable comments on an earlier draft of this manuscript. We also wish to thank to Centro de Supercomputación de Galicia (CESGA) for access to computer resources. VN was supported by a FPI pre-doctoral fellowship (BES-2012-053741) from Ministerio de Economía y Competitividad (Spain). JO was supported by Severo Ochoa (SEV-2012-0262) and Ramón y Cajal (RYC-2013-12501) research fellowships. This work received financial support from research grants CGL2011-25053, CGL2014-54671-P and CGL2016-8742-R (Ministerio de Economía y Competitividad and European Social Fund), POII10-0197-0167 and PEII-2014023-P (Junta de Comunidades de Castilla-La Mancha and European Social Fund) and UNCM08-1E-018 (European Regional Development Fund).

Appendix A. Supplementary material

Supplementary data associated with this article can be found, in the online version, at <http://dx.doi.org/10.1016/j.ympev.2017.10.012>.

References

- Abellán, P., Svenning, J.-C., 2014. Refugia within refugia – patterns in endemism and genetic divergence are linked to Late Quaternary climate stability in the Iberian Peninsula. *Biol. J. Linn. Soc.* 113, 13–28.
- Aljanabi, S.M., Martinez, I., 1997. Universal and rapid salt-extraction of high quality genomic DNA for PCR-based techniques. *Nucl. Acids Res.* 25, 4692–4693.
- Anderson, R.P., Raza, A., 2010. The effect of the extent of the study region on GIS models of species geographic distributions and estimates of niche evolution: preliminary tests with montane rodents (genus *Nephelomys*) in Venezuela. *J. Biogeogr.* 37, 1378–1393.
- Anthos, 2016. Sistema de información de las plantas de España. Real Jardín Botánico, CSIC-Fundación Biodiversidad. <https://www.anthos.es> (accessed 15.06. 2016).
- Andersen, J.C., Havill, N.P., Caccone, A.J.S., 2017. Postglacial recolonization shaped the genetic diversity of the winter moth (*Operophtera brumata*) in Europe. *Ecol. Evol.* 7, 3312–3323.
- Araújo, M.B., Peterson, T., 2012. Uses and misuses of bioclimatic envelope modeling. *Ecology* 93, 1527–1539.
- Arenas, M., Ray, N., Currat, M., Excoffier, L., 2012. Consequences of range contractions and range shifts on molecular diversity. *Mol. Biol. Evol.* 29, 207–218.
- Arnold, T.W., 2010. Uninformative parameters and model selection using Akaike's Information criterion. *J. Wildlife Manage.* 74, 1175–1178.
- Ashcroft, M.B., 2010. Identifying refugia from climate change. *J. Biogeogr.* 37, 1407–1413.
- Baele, G., Lemey, P., Bedford, T., Rambaut, A., Suchard, M.A., Alekseyenko, A.V., 2012. Improving the accuracy of demographic and molecular clock model comparison while accommodating phylogenetic uncertainty. *Mol. Biol. Evol.* 29, 2157–2167.
- Barton, K., 2015. MuMIn: multimodel Inference. R Package, version 1.15.6. <https://cran.r-project.org/web/packages/MuMIn/index.html>.
- Basita, R.K., Henrich Bruggemann, J., Cai, N., Cáliz-Campal, C., Chen, C., Chen, J., Cizek, L., Cordero, P.J., Dawson, D.A., Ding, Y., Drag, L., Duan, A., Fogliani, B., Gao, T.-X., Gélín, P., Genner, M.J., Gu, Z.-M., Guillaume, M.M.M., Guo, J.-L., He, C., Hollingsworth, P.M., Horsburgh, G.J., Inoue-Murayama, M., Ito, H., Jerry, D.R., Jia, Y.-Y., Jiang, W.-P., Jones, C.S., Jones, D.B., Kong, L., Li, Q., Li, C.-H., Li, X.-L., Li, J., Li, X., Lian, Q.-P., Lieber, L., Liu, L., Liu, S.-L., Liu, M., Luo, S., Maeda, T., Magalon, H., Martin, R.M., Mehn, V., Meyza, K., Noble, L.R., Noguerales, V., Ogdén, R., Oleksa, A., Onuma, M., Ortego, J., Pan, Y., Robinson, M.L., Rougeux, C., Ruhsam, M., Sato, Y., Song, N., Su, X., Sungani, H., Tao, P., Tian, B., Tian, J., Wang, R., Wang, X., Wang, X., Wang, D., Wilson, W.D., Wu, M., Wu, X., Wulff, A.S., Xu, Y., Xu, Y., Yanagimoto, T., Yin, S., Yu, H., Zeng, B., Zenger, K.R., Zhang, G., Zhao, J.-L., Zhou, Y., 2016. Erratum to: Microsatellite records for volume 7, issue 4. *Conserv. Genet. Resour.* 8, 85–87.
- Bates, D., Maechler, M., Bolker, B.M., Walker, S.C., 2015. Fitting linear mixed-effects models using lme4. *J. Stat. Softw.* 67, 1–48.
- Beaumont, M.A., 2010. Approximate Bayesian computation in evolution and ecology. *Annu. Rev. Ecol. Evol.* 41, 379–406.
- Bidegaray-Batista, L., Sánchez-Gracia, A., Santulli, G., Maiorano, L., Guisan, A., Vogler, A.P., Arnedo, M.A., 2016. Imprints of multiple glacial refugia in the Pyrenees revealed by phylogeography and palaeodistribution modelling of an endemic spider. *Mol. Ecol.* 25, 2046–2064.
- Borer, M., Arrigo, N., Buerki, S., Naisbit, R.E., Alvarez, N., 2012. Climate oscillations and species interactions: large-scale congruence but regional differences in the phylogeographic structures of an alpine plant and its monophagous insect. *J. Biogeogr.* 39, 1487–1498.
- Braconnot, P., Otto-Bliesner, B., Harrison, S., Joussaume, S., Peterchmitt, J.Y., Abe-Ouchi, A., Crucifix, M., Driesschaert, E., Fichefet, T., Hewitt, C.D., Kageyama, M., Kitoh, A., Laine, A., Loutre, M.F., Marti, O., Merkel, U., Ramstein, G., Valdes, P., Weber, S.L., Yu, Y., Zhao, Y., 2007. Results of PMIP2 coupled simulations of the Mid-Holocene and Last Glacial Maximum – part 1: experiments and large-scale features. *Clim. Past* 3, 261–277.
- Burnham, K.P., Anderson, D.R., 2002. Model Selection and Multi-Model Inference: A Practical Information-Theoretic Approach. Springer-Verlag, New York.
- Canestrelli, D., Cimmaruta, R., Costantini, V., Nascetti, G., 2006. Genetic diversity and phylogeography of the Apennine yellow-bellied toad *Bombina pachypus*, with implications for conservation. *Mol. Ecol.* 15, 3741–3754.
- Cangi, N., Horak, I.G., Apanaskevich, D.A., Matthee, S., das Neves, L.C.B.G., Estrada-Pena, A., Matthee, C.A., 2013. The influence of interspecific competition and host preference on the phylogeography of two African *Ixodid* tick species. *PLoS ONE* 8, e796930.
- Carnaval, A.C., Hickerson, M.J., Haddad, C.F.B., Rodrigues, M.T., Moritz, C., 2009. Stability predicts genetic diversity in the Brazilian Atlantic forest hotspot. *Science* 323, 785–789.
- Collins, W.D., Bitz, C.M., Blackmon, M.L., Bonan, G.B., Bretherton, C.S., Carton, J.A., Chang, P., Doney, S.C., Hack, J.J., Henderson, T.B., Kiehl, J.T., Large, W.G., McKenna, D.S., Santer, B.D., Smith, R.D., 2006. The Community Climate System Model version 3 (CCSM3). *J. Climate* 19, 2122–2143.
- Cooper, S.J.B., Hewitt, G.M., 1993. Nuclear DNA sequence divergence between parapatric subspecies of the grasshopper *Chorthippus parallelus*. *Insect Mol. Biol.* 2, 185–194.
- Cooper, S.J.B., Ibrahim, K.M., Hewitt, G.M., 1995. Postglacial expansion and genome subdivision in the European grasshopper *Chorthippus parallelus*. *Mol. Ecol.* 4, 49–60.
- Cornille, A., Giraud, T., Bellard, C., Tellier, A., Le Cam, B., Smulders, M.J.M., Kleinschmit, J., Roldan-Ruiz, I., Gladieux, P., 2013. Postglacial recolonization history of the European crabapple (*Malus sylvestris* Mill.), a wild contributor to the domesticated apple. *Mol. Ecol.* 22, 2249–2263.
- Cornuet, J.-M., Pudlo, P., Veysier, J., Dehne-Garcia, A., Gautier, M., Leblois, R., Marin, J.-M., Estoup, A., 2014. DIYABC v2.0: a software to make approximate Bayesian computation inferences about population history using single nucleotide polymorphism, DNA sequence and microsatellite data. *Bioinformatics* 30, 1187–1189.
- Criscione, C.D., Blouin, M.S., 2004. Life cycles shape parasite evolution: comparative population genetics of salmon trematodes. *Evolution* 58, 198–202.
- Chapuis, M.P., Estoup, A., 2007. Microsatellite null alleles and estimation of population differentiation. *Mol. Biol. Evol.* 24, 621–631.
- Darriba, D., Taboada, G.L., Doallo, R., Posada, D., 2012. jModelTest2: more models, new heuristics and parallel computing. *Nat. Methods* 9, 772–772.
- Defaut, B., 2011. Preliminary revision of *Chorthippus* of the *binotatus* group (Charpentier, 1825) (Caelifera, Acrididae, Gomphocerinae). *Materiaux Orthoptériques et Entomocénologiques* 16, 17–54.
- Drummond, A.J., Rambaut, A., Shapiro, B., Pybus, O.G., 2005. Bayesian coalescent inference of past population dynamics from molecular sequences. *Mol. Biol. Evol.* 22, 1185–1192.
- Drummond, A.J., Suchard, M.A., Xie, D., Rambaut, A., 2012. Bayesian phylogenetics with BEAST 1.7. *Mol. Biol. Evol.* 29, 1969–1973.
- Dupanloup, I., Schneider, S., Excoffier, L., 2002. A simulated annealing approach to define the genetic structure of populations. *Mol. Ecol.* 11, 2571–2581.
- Eckert, C.G., Samis, K.E., Loughheed, S.C., 2008. Genetic variation across species' geographical ranges: the central-marginal hypothesis and beyond. *Mol. Ecol.* 17, 1170–1188.
- Evanno, G., Regnaut, S., Goudet, J., 2005. Detecting the number of clusters of individuals using the software Structure: a simulation study. *Mol. Ecol.* 14, 2611–2620.
- Excoffier, L., Lischer, H.E.L., 2010. Arlequin suite ver 3.5: a new series of programs to perform population genetics analyses under Linux and Windows. *Mol. Ecol. Resour.* 10, 564–567.
- Excoffier, L., Ray, N., 2008. Surfing during population expansions promotes genetic revolutions and structuration. *Trends Ecol. Evol.* 23, 347–351.
- Falush, D., Stephens, M., Pritchard, J.K., 2003a. Inference of population structure using multilocus genotype data: linked loci and correlated allele frequencies. *Genetics* 164, 1567–1587.
- Falush, D., Wirth, T., Linz, B., Pritchard, J.K., Stephens, M., Kidd, M., Blaser, M.J., Graham, D.Y., Vacher, S., Pérez-Pérez, G.I., Yamaoka, Y., Mégraud, F., Otto, K., Reichard, U., Katzwitsch, E., Wang, X., Achtman, M., Suerbaum, S., 2003b. Traces of human migrations in *Helicobacter pylori* populations. *Science* 299, 1582–1585.
- Falush, D., van Dorp, L., Lawson, D., 2016. A tutorial on how (not) over-interpret Structure/Admixture barplots. [bioRxiv, http://dx.doi.org/10.1101/066431](http://dx.doi.org/10.1101/066431).
- Faye, A., Deblauwe, V., Mariac, C., Richard, D., Sonke, B., Vigouroux, Y., Couvreur, T.L.P., 2016. Phylogeography of the genus *Podococcus* (Palmae/Arecaceae) in Central African rain forests: climate stability predicts unique genetic diversity. *Mol. Phylogenet. Evol.* 105, 126–138.
- Felsenstein, J., 2013. PHYLIP (Phylogeny Inference Package) version 3.695. Department of Genome Sciences, University of Washington, Seattle. <http://evolution.genetics.washington.edu/phylip.html>.
- Folmer, O., Black, M., Hoeh, W., Lutz, R., Vrijenhoek, R., 1994. DNA primers for amplification of mitochondrial cytochrome c oxidase subunit I from diverse metazoan invertebrates. *Mol. Mol. Mar. Biol. Biotech.* 3, 294–299.
- Fontaine, M.C., Austerlitz, F., Giraud, T., Labbé, F., Papura, D., Richard-Cervera, S., Delmotte, F., 2013. Genetic signature of a range expansion and leap-frog event after the recent invasion of Europe by the grapevine downy mildew pathogen *Plasmopara viticola*. *Mol. Ecol.* 22, 2771–2786.
- François, O., 2016. Running Structure-like population genetic analyses with R. R Tutorials in Population Genetics, U. Grenoble-Alpes. <http://membres-timc.imag.fr/Olivier.Francois/tutoRstructure.pdf>.
- Freeman, B.G., Mason, N.A., 2015. The geographic distribution of a tropical montane bird is limited by a tree: acorn woodpeckers (*Melanerpes formicivorus*) and Colombian Oaks (*Quercus humboldtii*) in the Northern Andes. *PLoS ONE* 10, e0128675.
- Fu, Y.X., 1997. Statistical tests of neutrality of mutations against population growth, hitchhiking and background selection. *Genetics* 147, 915–925.
- Galbreath, K.E., Hafner, D.J., Zamudio, K.R., 2009. When cold is better: climate-driven elevation shifts yield complex patterns of diversification and demography in an alpine specialist (American Pika, *Ochotona princeps*). *Evolution* 63, 2848–2863.
- Gómez, A., Lunt, D.H., 2007. Refugia within refugia: patterns of phylogeographic concordance in the Iberian Peninsula. In: Weiss, S., Ferrand, N. (Eds.), *Phylogeography in Southern European Refugia: Evolutionary Perspectives on the Origins and Conservation of European Biodiversity*. Springer Verlag, Dordrecht, The Netherlands, pp. 155–188.
- Grant, W.S., 2015. Problems and cautions with sequence mismatch analysis and Bayesian Skyline Plots to infer historical demography. *J. Hered.* 106, 333–346.
- Guo, Q., 2012. Incorporating latitudinal and central-marginal trends in assessing genetic variation across species ranges. *Mol. Ecol.* 21, 5396–5403.
- Gutiérrez-Rodríguez, J., Barbosa, A.M., Martínez-Solano, I., 2016. Present and past climatic effects on the current distribution and genetic diversity of the Iberian spadefoot toad (*Pelobates cultripes*): an integrative approach. *J. Biogeogr.* 44, 245–258.
- Hampe, A., 2004. Bioclimate envelope models: what they detect and what they hide. *Global Ecol. Biogeogr.* 13, 469–471.
- Harpending, H.C., 1994. Signature of ancient population-growth in a low-resolution mitochondrial-DNA mismatch distribution. *Hum. Biol.* 66, 591–600.
- Harter, A.V., Gardner, K.A., Falush, D., Lentz, D.L., Bye, R.A., Rieseberg, L.H., 2004. Origin of extant domesticated sunflowers in eastern North America. *Nature* 430,

- 201–205.
- Hewitt, G., 2000. The genetic legacy of the Quaternary ice ages. *Nature* 405, 907–913.
- Hewitt, G.M., 1996. Some genetic consequences of ice ages, and their role in divergence and speciation. *Biol. J. Linn. Soc.* 58, 247–276.
- Hewitt, G.M., 1999. Post-glacial re-colonization of European biota. *Biol. J. Linn. Soc.* 68, 87–112.
- Hewitt, G.M., 2004a. Genetic consequences of climatic oscillations in the Quaternary. *Philos. T. Roy. Soc. B* 359, 183–195.
- Hewitt, G.M., 2004b. The structure of biodiversity – insights from molecular phylogeography. *Front. Zool.* 1, 1–16.
- Hewitt, G.M., 2011. Quaternary phylogeography: the roots of hybrid zones. *Genetica* 139, 617–638.
- Hickerson, M.J., Cunningham, C.W., 2005. Contrasting quaternary histories in an ecologically divergent sister pair of low-dispersing intertidal fish (*Xiphister*) revealed by multilocus DNA analysis. *Evolution* 59, 344–360.
- Hijmans, R.J., Cameron, S.E., Parra, J.L., Jones, P.G., Jarvis, A., 2005. Very high resolution interpolated climate surfaces for global land areas. *Int. J. Climatol.* 25, 1965–1978.
- Hijmans, R.J., van Etten, J., 2016. Raster: geographic analysis and modeling with raster data. R package version 2.5-8. <http://CRAN.R-project.org/package=raster>.
- Ho, S.Y.W., Shapiro, B., 2011. Skyline-plot methods for estimating demographic history from nucleotide sequences. *Mol. Ecol. Resour.* 11, 423–434.
- Hutchinson, G.E., 1957. Concluding remarks. In: *Cold Spring Harbor Symposia on Quantitative Biology*, vol. 22, pp. 415–427.
- Inoue, K., Lang, B.K., Berg, D.J., 2015. Past climate change drives current genetic structure of an endangered freshwater mussel species. *Mol. Ecol.* 24, 1910–1926.
- Jackson, S.T., Overpeck, J.T., 2000. Responses of plant populations and communities to environmental changes of the late Quaternary. *Paleobiology* 26, 194–220.
- Jakobsson, M., Rosenberg, N.A., 2007. CLUMPP: a cluster matching and permutation program for dealing with label switching and multimodality in analysis of population structure. *Bioinformatics* 23, 1801–1806.
- Jay, F., Manel, S., Alvarez, N., Durand, E.Y., Thuiller, W., Holderegger, R., Taberlet, P., François, O., 2012. Forecasting changes in population genetic structure of alpine plants in response to global warming. *Mol. Ecol.* 21, 2354–2368.
- Kalinowski, S.T., 2005. HP-Rare 1.0: a computer program for performing rarefaction on measures of allelic richness. *Mol. Ecol. Notes* 5, 187–189.
- Keppel, G., Van Niel, K.P., Wardell-Johnson, G.W., Yates, C.J., Byrne, M., Mucina, L., Schut, A.G.T., Hopper, S.D., Franklin, S.E., 2012. Refugia: identifying and understanding safe havens for biodiversity under climate change. *Global Ecol. Biogeogr.* 21, 393–404.
- Kuhn, T., Cunze, S., Kochman, J., Limpel, S., 2016. Environmental variable and definitive host-distribution: a habitat suitability modelling for endohelminth parasites in the marine realm. *Sci. Rep.* 6, 30246.
- Laukkanen, L., Mutikainen, P., Muola, A., Leimu, R., 2014. Plant-species diversity correlates with genetic variation of an oligophagous seed predator. *PLoS ONE* 9, e94105.
- Leigh, J.W., Bryant, D., 2015. PopART: full-feature software for haplotype network construction. *Methods Ecol. Evol.* 6, 1110–1116.
- Librado, P., Rozas, J., 2009. DnaSP v5: a software for comprehensive analysis of DNA polymorphism data. *Bioinformatics* 25, 1451–1452.
- Liu, C.R., Berry, P.M., Dawson, T.P., Pearson, R.G., 2005. Selecting thresholds of occurrence in the prediction of species distributions. *Ecography* 28, 385–393.
- Llucià-Pomares, D., 2002. Revision of the Orthoptera (Insecta) of Catalonia (Spain). Zaragoza, Spain.
- Massatti, R., Knowles, L.L., 2016. Contrasting support for alternative models of genomic variation based on microhabitat preference: species-specific effects of climate change in alpine sedges. *Mol. Ecol.* 25, 3974–3986.
- Mouritsen, K.N., Poulin, R., 2002. Parasitism, climatic oscillations and the structure of natural communities. *Oikos* 97, 462–468.
- Noguerales, V., Cordero, P.J., Ortego, J., 2016a. Hierarchical genetic structure shaped by topography in a narrow-endemic montane grasshopper. *BMC Evol. Biol.* 16, 96.
- Noguerales, V., Cordero, P.J., Ortego, J., 2017. Testing the role of ancient and contemporary landscapes on structuring genetic variation in a specialist grasshopper. *Ecol. Evol.* 7, 3110–3122.
- Noguerales, V., García-Navas, V., Cordero, P.J., Ortego, J., 2016b. The role of environment and core-margin effects on range-wide phenotypic variation in a montane grasshopper. *J. Evol. Biol.* 29, 2129–2142.
- Noguerales, V., Traba, J., Mata, C., Morales, M., 2015. Winter habitat selection and partitioning in two sympatric farmland small mammals: *Apodemus sylvaticus* and *Mus spretus*. *Revue d'écologie (La Terre et la Vie)* 70, 70–82.
- Nogués-Bravo, D., 2009. Predicting the past distribution of species climatic niches. *Global Ecol. Biogeogr.* 18, 521–531.
- Ortego, J., Aguirre, M.P., Noguerales, V., Cordero, P.J., 2015a. Consequences of extensive habitat fragmentation in landscape-level patterns of genetic diversity and structure in the Mediterranean esparto grasshopper. *Evol. Appl.* 8, 621–632.
- Ortego, J., Noguerales, V., Guggler, P.F., Sork, V.L., 2015b. Evolutionary and demographic history of the Californian scrub white oak species complex: an integrative approach. *Mol. Ecol.* 24, 6188–6208.
- Papadopoulou, A., Anastasiou, I., Vogler, A.P., 2010. Revisiting the insect mitochondrial molecular clock: the Mid-Aegean trench calibration. *Mol. Biol. Evol.* 27, 1659–1672.
- Parducci, L., Jorgensen, T., Tollefsrud, M.M., Elverland, E., Alm, T., Fontana, S.L., Bennett, K.D., Haile, J., Matetovici, I., Suyama, Y., Edwards, M.E., Andersen, K., Rasmussen, M., Boessenkool, S., Coissac, E., Brochmann, C., Taberlet, P., Houmark-Nielsen, M., Larsen, N.K., Orlando, L., Gilbert, M.T.P., Kjaer, K.H., Alsos, I.G., Willerslev, E., 2012. Glacial survival of boreal trees in Northern Scandinavia. *Science* 335, 1083–1086.
- Peterson, A.T., Soberon, J., Sanchez-Cordero, V., 1999. Conservatism of ecological niches in evolutionary time. *Science* 285, 1265–1267.
- Petit, J.R., Jouzel, J., Raynaud, D., Barkov, N.I., Barnola, J.M., Basile, I., Bender, M., Chappellaz, J., Davis, M., Delaygue, G., Delmotte, M., Kotlyakov, V.M., Legrand, M., Lipenkov, V.Y., Lorius, C., Pepin, L., Ritz, C., Saltzman, E., Stievenard, M., 1999. Climate and atmospheric history of the past 420,000 years from the Vostok ice core, Antarctica. *Nature* 399, 429–436.
- Phillips, S.J., Anderson, R.P., Schapire, R.E., 2006. Maximum entropy modeling of species geographic distributions. *Ecol. Model.* 190, 231–259.
- Phillips, S.J., Dudik, M., 2008. Modeling of species distributions with Maxent: new extensions and a comprehensive evaluation. *Ecography* 31, 161–175.
- Picaud, F., Bonnet, E., Gloaguen, V., Petit, D., 2003. Decision making for food choice by grasshoppers (Orthoptera: Acrididae): comparison between a specialist species on a shrubby legume and three gaminivorous species. *Environ. Entomol.* 32, 680–688.
- Picaud, F., Gloaguen, V., Petit, D., 2002. Mechanistic aspects to feeding preferences in *Chorthippus binotatus* (Acrididae: Gomphocerinae). *J. Insect Behav.* 15, 513–526.
- Platz, J., Cloupeau, R., 2010. Liste rouge commentée des Orthopères de la région Centre. *Matériaux Orthopédiques et Entomocénétiques* 15, 17–33.
- Pritchard, J.K., Stephens, M., Donnelly, P., 2000. Inference of population structure using multilocus genotype data. *Genetics* 155, 945–959.
- Pritchard, J.K., Wen, X., Falush, D., 2010. Documentation for Structure Software: version 2.3. <http://pritchardlab.stanford.edu/structure.html>.
- Provan, J., Bennett, K.D., 2008. Phylogeographic insights into cryptic glacial refugia. *Trends Ecol. Evol.* 23, 564–571.
- Qu, Y., Ericson, P.G.P., Quan, Q., Song, G., Zhang, R., Gao, B., Lei, F., 2014. Long-term isolation and stability explain high genetic diversity in the Eastern Himalaya. *Mol. Ecol.* 23, 705–720.
- R Core Team, 2015. R: A Language and Environment for Statistical Computing. R Foundation for Statistical Computing, Vienna, Austria. <http://www.R-project.org/>.
- Ramos-Onsins, S.E., Rozas, J., 2002. Statistical properties of new neutrality tests against population growth. *Mol. Biol. Evol.* 19, 2092–2100.
- Ricanova, S., Koshev, Y., Rican, O., Cosic, N., Cirovic, D., Sedlacek, F., Bryja, J., 2013. Multilocus phylogeography of the European ground squirrel: cryptic interglacial refugia of continental climate in Europe. *Mol. Ecol.* 22, 4256–4269.
- Rice, W.R., 1989. Analyzing tables of statistical tests. *Evolution* 43, 223–225.
- Rogers, A.R., Harpending, H., 1992. Population-growth makes waves in the distribution of pairwise genetic-differences. *Mol. Biol. Evol.* 9, 552–569.
- Rosenberg, N.A., 2004. DISTRUCT: a program for the graphical display of population structure. *Mol. Ecol. Notes* 4, 137–138.
- Salvi, D., James Harris, D., Kaliontzopoulou, A., Carretero, M.A., Pinho, C., 2013. Persistence across Pleistocene ice ages in Mediterranean and extra-Mediterranean refugia: phylogeographic insights from the common wall lizard. *BMC Evol. Biol.* 13, 147.
- Schmitt, T., 2007. Molecular biogeography of Europe: Pleistocene cycles and postglacial trends. *Front. Zool.* 4, 11.
- Schmitt, T., Varga, Z., 2012. Extra-Mediterranean refugia: the rule and not the exception? *Front. Zool.* 9, 11.
- Schneider, S., Excoffier, L., 1999. Estimation of past demographic parameters from the distribution of pairwise differences when the mutation rates vary among sites: application to human mitochondrial DNA. *Genetics* 152, 1079–1089.
- Schweiger, O., Settele, J., Kudrna, O., Klotz, S., Kuhn, I., 2008. Climate change can cause spatial mismatch of trophically interacting species. *Ecology* 89, 3472–3479.
- Shaw, A.J., Shaw, B., Stenøien, H.K., Golinski, G.K., Hassel, K., Flatberg, K.L., 2015. Pleistocene survival, regional genetic structure and interspecific gene flow among three northern peat-mosses: *Sphagnum inexpectatum*, *S. orientale* and *S. miyabeumum*. *J. Biogeogr.* 42, 364–376.
- Snyder, C.W., 2016. Evolution of global temperature over the past two million years. *Nature* 538, 226–228.
- Stewart, J.R., Lister, A.M., 2001. Cryptic northern refugia and the origins of the modern biota. *Trends Ecol. Evol.* 16, 608–613.
- Stewart, J.R., Lister, A.M., Barnes, I., Dalen, L., 2010. Refugia revisited: individualistic responses of species in space and time. *Proc. R. Soc. B* 277, 661–671.
- Svenning, J.-C., Flojgaard, C., Marske, K.A., Nogués-Bravo, D., Normand, S., 2011. Applications of species distribution modeling to paleobiology. *Quat. Sci. Rev.* 30, 2930–2947.
- Taberlet, P., Fumagalli, L., Wust-Saucy, A.G., Cosson, J.F., 1998. Comparative phylogeography and postglacial colonization routes in Europe. *Mol. Ecol.* 7, 453–464.
- Tajima, F., 1989. Statistical-method for testing the neutral mutation hypothesis by DNA polymorphism. *Genetics* 123, 585–595.
- Talavera, S., Aedo, C., Castroviejo, S., Romero, C., Sáez, L., Salgueiro, F.J., Velayos, M., 2001. Flora Ibérica VII/1 Leguminosae (partim). Real Jardín Botánico, CSIC, Madrid.
- Tsai, Y.-H.E., Manos, P.S., 2010. Host density drives the postglacial migration of the tree parasite, *Epifagus virginiana*. *Proc. Natl. Acad. Sci. USA* 107, 17035–17040.
- Tsuda, Y., Nakao, K., Ide, Y., Tsumura, Y., 2015. The population demography of *Betula maximowicziana*, a cool-temperate tree species in Japan, in relation to the last glacial period: its admixture-like genetic structure is the result of simple population splitting not admixing. *Mol. Ecol.* 24, 1403–1418.
- Ursenbacher, S., Guillon, M., Cubizolle, H., Dupoué, A., Blouin-Demers, G., Lourdaux, O., 2015. Postglacial recolonization in a cold climate specialist in western Europe: patterns of genetic diversity in the adder (*Vipera berus*) support the central-marginal hypothesis. *Mol. Ecol.* 24, 3639–3651.
- Vega, R., Flojgaard, C., Lira-Noriega, A., Nakazawa, Y., Svenning, J.-C., Searle, J.B., 2010. Northern glacial refugia for the pygmy shrew *Sorex minutus* in Europe revealed by phylogeographic analyses and species distribution modelling. *Ecography* 33, 260–271.
- Warren, D.L., Glor, R.E., Turelli, M., 2010. ENMTools: a toolbox for comparative studies

- of environmental niche models. *Ecography* 33, 607–611.
- Warren, D.L., Seifert, S.N., 2011. Ecological niche modeling in Maxent: the importance of model complexity and the performance of model selection criteria. *Ecol. Appl.* 21, 335–342.
- Wharton, T.N., Kriticos, D.J., 2004. The fundamental and realized niche of the Monterey Pine aphid, *Essigella californica* (Essig) (Hemiptera: Aphididae): implications for managing softwood plantations in Australia. *Divers. Distrib.* 10, 253–262.
- Willis, K.J., van Andel, T.H., 2004. Trees or no trees? The environments of central and eastern Europe during the Last Glaciation. *Quat. Sci. Rev.* 23, 2369–2387.
- Wachter, G.A., Papadopoulou, A., Muster, C., Arthofer, W., Knowles, L.L., Steiner, F.M., Schlick-Steiner, B.C., 2016. Glacial refugia, recolonization patterns and diversification forces in Alpine-endemic *Megabumus* harvestmen. *Mol. Ecol.* 25, 2904–2919.
- Yannic, G., Pellissier, L., Ortego, J., Lecomte, N., Couturier, S., Cuyler, C., Dussault, C., Hundertmark, K.J., Irvine, R.J., Jenkins, D.A., Kolpashikov, L., Mager, K., Musiani, M., Parker, K.L., Roed, K.H., Sipko, T., Porisson, S.G., Weckworth, B.V., Guisan, A., Bernatchez, L., Cote, S.D., 2014. Genetic diversity in caribou linked to past and future climate change. *Nat. Clim. Change* 4, 132–137.